ISSN: 2716-9227 Algerian Journal of Engineering and Technology 08 (2023) 272–276 e-ISSN: 2716-9278

Algerian Journal of Engineering and Technology

Journal homepage: https://jetjournal.org/index.php/ajet

Original Article

Al 6061-T6 microstructure and mechanical properties modification under ion beam irradiation at room temperature: Application for Nuclear Research Reactor

Mahmoud Izerrouken [a]*, Ali Sari [b], Omar Menchi[a], Fadila Haid[c] and Ahmed Ishaq[d]

[a]*Nuclear Research Center of Draria, Bp. 43 Sebbala, Draria, Algiers, Algeria.*
[b]*Nuclear research center of Birine, BP 108, Ain-Oussera, Djelfa, Algeria*
[c]*Development Centre of Advanced Technologies, 20 August city 1956, Bp. 17, Baba Hassen, Algiers, Algeria*
[d]*National Centre for Physics (NCP), Islamabad, Pakistan*

ARTICLE INFO

Article history:
Received 23 July 2023
Revised 25 October 2023
Accepted 28 October 2023

Keywords:
Aluminium alloys;
Mechanical properties;
Radiation damage;
Vacancy clusters;
Interstitial clusters;
Radiation hardening.

ABSTRACT

Al6061 microstructural and mechanical properties modification under ion beam irradiation was investigated using X-ray diffraction (XRD), micro- and nano-indentation techniques. The samples were irradiated with different ions species at different energies and doses. The irradiations were performed at 5UDH-2 Pelletron Tandem accelerator Islamabad, Pakistan and GANIL accelerator, Caen, France. XRD patterns show a drastic effect of ion beam irradiation on the peaks intensity. All peaks disappear after irradiation except the peak (200) and new phase/precipitates emerged at high doses. It is found that the grain size, micro-strain and peaks shift increase/or decrease depending on the ion species and dose. The micro-hardness increases a little bit after irradiation indicating Al6061 hardening by ion beam irradiation. The result of this study demonstrated that the structure and microstructure of Al6061 are significantly changed by heavy ion irradiation. This will affect certainly the Al6061 mechanical properties and, therefore, reduces its lifetime under reactor neutron operation conditions.

1. Introduction

Aluminum based alloys have found the greatest use in nuclear industry, as a cladding and structural materials for nuclear reactor fuel assembly due to their favorable mechanical properties at low temperature (research reactor temperature operation) and its low neutron absorption cross-section (0.23 barns) [1, 2]. Al 6061-T6 particularly presents successful stability of its properties under irradiation compared to other alloys. Furthermore, more than 50% of operating research reactors are over 45 years old, and more than 30% are over 50 years old. Thus, aging management for the core structural components becomes one of the key issues. However, given the needs for radioisotopes, few countries have increased the power of their reactors and extended their lifetime. Thus, a structured database is required to understand the material behavior in core components of research reactors for their continued safe operation and lifetime extension [3]. The prediction of its mechanical properties during service becomes important for safety and security of the nuclear installation.

Most studies revealed fast and thermal neutrons irradiation induced Si precipitates which causes aluminum alloy swelling, cavities formation and sample hardening. For instance K. Farrell and R. King [4] revealed the formation of about 7wt% Si from the transmutation reaction, voids causing a swelling less than 1% and an increase in the ultimate tensile strength (UTS) of about 60% in Al 6061-T6 irradiated at 50°C at a fast neutrons (E>0.1 MeV) of 1.8×10^{23} n.cm^{-2} and thermal neutrons (0.025 eV) of 3×10^{23} n.cm^{-2}. More detailed studies of radiation damage in

* *Corresponding author* :.
E-mail address: *m-izerrouken@crnd.dz*
Peer review under responsibility of University of El Oued.
 https://dx.doi.org/10.57056/ajet.v8i2.133

aluminum alloys have been carried out using ion beam irradiation to understand the evolution of microstructure and hardness and their possible correlation. Indeed, ion beam is one way used actually in several laboratories to emulate neutron radiation damage due mainly to high displacement damage rate and very low radioactivity. It has been reported that the, β'' (Mg_5Si_6) precipitates are completely dissolved, the new phase has grown and a high density of clusters rich in Mg, Si, Cu and Cr is observed in Al6061-T6 irradiated by 2 MeV W^{+3} and 4 MeV Au^{+2} ions at a dose of 165 dpa [5]. This precipitates dissolution is attributed to the irradiation-enhanced diffusion and the new phases to the irradiation induced segregation. Likewise, D. Ueyama et al. [6] study revealed that Al-Mg-Si alloys irradiated by Al, Fe, I and Au ions of 5.4, 7.3, 10 and 16 MeV respectively increase the hardness and reach a saturation value at high fluence (>10^{15} ions.cm^{-2}). The authors conclude that the change in Vickers hardness is well correlated with the deposited energy density through the elastic collision. Besides numerous studies, the mechanism of radiation damage and the correlation between defect formation and change in mechanical properties are still poorly understood. In this work, the modification of structural and mechanical properties under several ions species of different energies and doses were investigated using X-ray diffraction (XRD), nano-indentation and micro-indentation techniques.

2. Materials and Methods

The samples investigated in this study are from two different provenances noted Al6061 (P1) and Al6061(P2). The chemical composition of the main elements is 0.4 wt% Si, 0.8 wt% Mg, 0.15 wt% Cu, 0.04 wt% Cr and 98.61wt% Al. Small pieces with size of about 10 mm x 10 mm, were cut from the same plate by a diamond saw. The surface of the samples was mechanically polished using SiC paper (grits 200–1500), then cleaned in acetone and ethanol, and finally washed in water. The samples Al6061(P1) were irradiated with Ar ion of 165 keV, while Al6061(P2) were irradiated with Cu ion of 700 keV and 20 MeV and, Au ion of 3 MeV and 20 MeV. Ar^{2+} irradiation was performed at room temperature at GANIL accelerator, Caen, France. Cu and Au irradiations were performed at National Center of Physics, Islamabad, Pakistan using 5UDH-2 Pelletron Tandem accelerator. The irradiations were carried out at room temperature in a vacuum chamber at 3 ×10^{-7} torr and irradiation current varied from 50 nm to 90 nA. In both irradiation experiments a small part of each sample was masked by aluminum foil to be served as a reference part. The detailed irradiation parameters are reported in table 1 where the electronic stopping power S_e, nuclear stopping power S_n and projected ion range R_p were calculated using SRIM (Stopping and Range of Ions in Matter) 2003 code [7]. The number of displacements per atom (dpa) was calculated using eq. 1 [8].

$$n_{dpa} = \frac{\phi . N_d . A}{\rho . d . N_A} \quad (1)$$

where ϕ is the ion fluence, N_d is the number of displacements per ion, A is the molecular mass of the target material, ρ is the density, d is the penetration depth, N_A is Avogadro's number. The displacement damage (N_d/d) was calculated using SRIM 2003 code with ''quick damage calculation'' mode and using displacement energy threshold of 25 eV for Al. The dpa values corresponding to each fluence obtained at the maximum of the dpa distribution are reported in Table 1.

After irradiation the structure modifications are observed using XRD, X' PERT PRO MPD in the Bragg–Brentano geometry: The X-ray source was a copper tube (CuKa = 1.540,598 A°) and a PIXcel 1D detector was used for X-ray detection. The 2h scan range was 20° - 80 ° with a step size of 0.026°. The mechanical tests were performed using micro-durometer INNOVATEST FALCON 400. The measurements were performed using Vickers indenter with loads of 0.1 N (10 g) and load time of 10 s.The modification on nano-mechanical property was studied using nanoindentation test. The measurements were carried out using a continuous stiffness measurement (CSM) mode with a Berkovich diamond indenter at room temperature. A maximum load of 3.5 mN and a loading time of 10 s were applied for each sample. In order to obtain accurate statistical data, different indents were performed on each sample with 0.15 mm spacing between each indent. The nano-hardness (H) and Young's modulus (E) values were determined using the Oliver-Pharr method [9].

Table 1: Irradiation parameters.

Ion/Energy MeV	Se keV/µm	Sn keV/µm	Rp µm	Fluence Ion/cm^2	Dose dpa
Ar/ 0.165	0.63	0.45	0.144	2×10^{14}	0.2
				5×10^{14}	0.5
				10×10^{14}	1.1
				20×10^{14}	2.2
				30×10^{14}	3.3
Cu/0.7	0.64	0.62	0.500	1×10^{15}	1.4
				5×10^{15}	7.2
Cu/20	5.6	0.064	0.200	1×10^{15}	1.0
				5×10^{15}	4.8
Au/3	2.5	2.4	0.600	1×10^{15}	4.7
				5×10^{15}	23.0
Au/20	3.9	0.9	4.200	1×10^{15}	2.8
				5×10^{15}	14.2

3. Results and Discussion

3.1. Structural modification

Fig 1 shows the XRD patterns recorded for samples irradiated by 165 keV Ar ion, 20 MeV Cu ion, 3MeV Au ion and 20 MeV Au ion compared to the unirradiated sample. Both investigated samples exhibit a strong texture along (111), (200), (220), (311) and (222) diffraction peak corresponding to cubic structure of the samples according to PDF reference code 00-004-0787, athough they have different preferred orientation. After irradiation one can see a variation of the peak intensity indicating restructuration due to the defect formation.

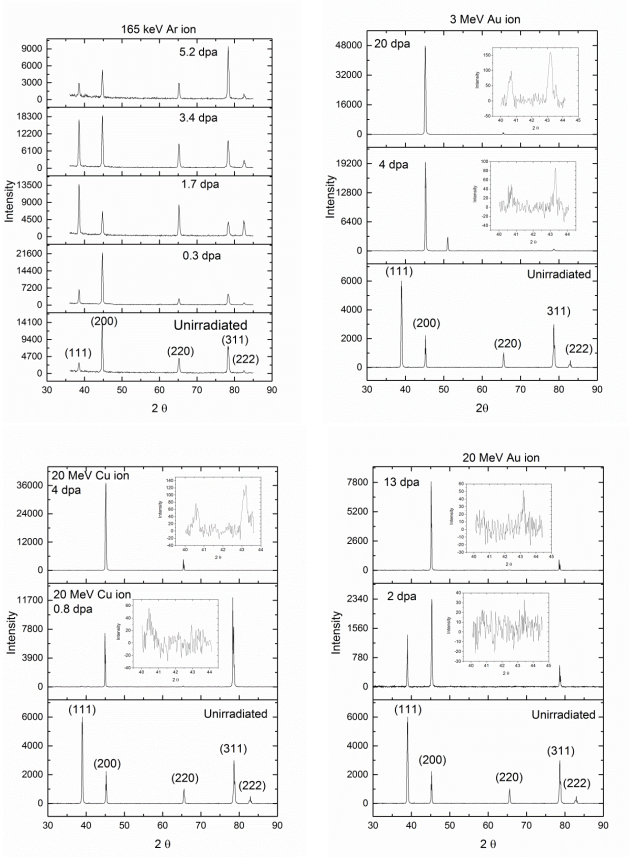

Fig1. XRD patterns of Al6061 irradiated by 165 keV Ar ion, 3 MeV and 20 MeV Au ion and, 20 MeV Cu ion at different doses compared to the unirradiated sample.

This is well illustrated in Fig.2 where the evolution of the I(200)/I(111) peak ratio were presented versus dose.

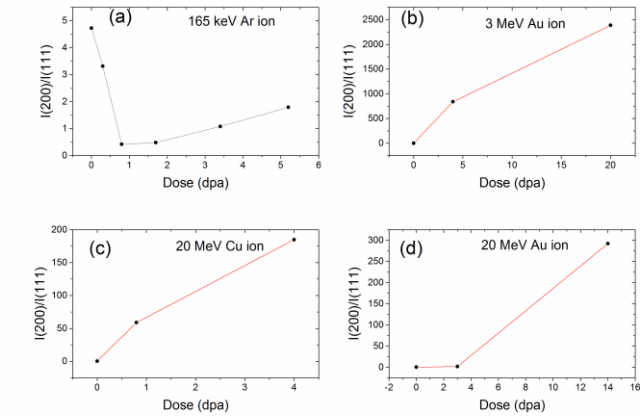

Fig 2. The evolution of the I(200)/I(111) peak ratio versus dose observed in Al6061 irradiated by 165 keV Ar ion, 3 MeV and 20 MeV Au ion and, 20 MeV Cu ion.

As can be seen, the I(200)/I(111) values decreases up to a critical dose of about 1 dpa and then increases monotonously with the dose in accordance with Abdel-Rahman et el. [10] results. The authors observed similar behavior as a function of deformation. A critical deformation value of 10.47% was reported. Moreover, at high doses, all peaks disappear except the peak (200). This indicates lattice distortion anisotropy, probably due to the displacement threshold energy variation along each plane direction. Exactly similar observation was made recently by San Chae et al [11] in pure Al irradiated by 18 MeV He^{+} ion up to a fluence of 1×10^{16} ions.cm^{-2}. They attributed the peak intensity trend to the defects generated in the form of exfoliational sputtering and re-deposition. Furthermore, the increase of the (200) peak intensity above 1 dpa is interpreted as an increase in the crystalline degree. However, it is interesting to note that the crystallite size, the micro-strain and the peaks shift towards lower angle associated with each orientation depends on the ion species and energy as was noticed in Ueyama et al. research [6]. So to check the defect formation mechanism, the I(200)/I(111) peak ratio normalize to the ion path obtained at the same dose of 4dpa was presented as a function of the nuclear stopping power (S_n) (see Fig. 3).

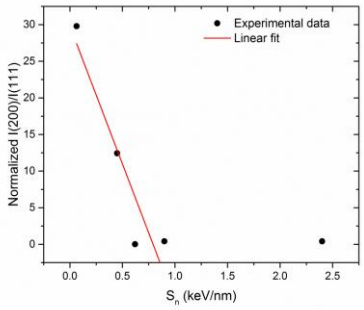

Fig 3. Normalized I(200)/I(111) peak ratio measured at about 4 dpa as a function of the nuclear topping power.

It is clear from the figure that perfect correlations exist between the peak ratio and the nuclear stopping power range lower than 1 keV/nm. Above this value the peak ratio reach saturation. Thus the displacive radiation damage is the main mechanism responsible of the defect formation in Aluminum alloys. The restructuration is then due to the point defect (PD) (vacancies and interstitials) generated by ion beam irradiation. With increasing dose PD concentration increases and annihilates in the extended sinks (grain size) which justify the saturation effect. At high doses, vacancies and interstitials in excess can form a complex with the solute element and drag it towards the PD sinks, which leads to solute enrichment mechanism known as radiation-induced segregation (RIS). The latter process may be explain the new peaks emerging at about 2θ=40.6° and 43.15 above a given dose depending on the ion species and energy. It is attributed to the new phase formation due to the segregation effect in accordance with earlier findings [5]. Indeed, it is well established that radiation-induced segregation is the main mechanism for solute enrichment or depletion on microstructural defects see ref [10] and references therein.

3.2. Mechanical property modification

Fig. 4a presents the comparison between the micro-hardness measured for unirradiated part and irradiated part for each ion species. The comparison reveals a small hardening after irradiation. The change in the micro-hardness calculated using equation 2 is depicted in Fig. 4 b.

$$\Delta H=(H-H_0)/H_0 \quad (2)$$

As can be seen, ΔH reaches a saturation value of about 7% at 3 dpa attributed to the defect recombination process as explained above.

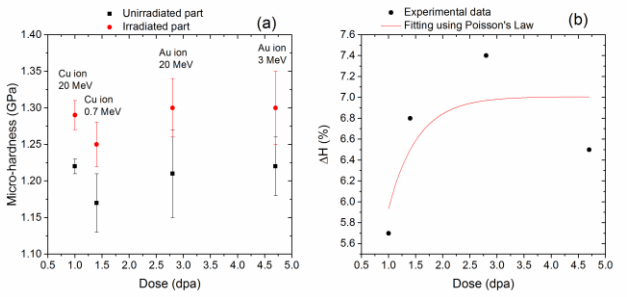

Fig. 4. (a) Comparison between the micro-hardness measured in unirradiated part and irradiated part for each sample. (b) Micro-hardness changes versus dose. The solid line is the fitting of the experimental data using Poisson's law.

The results of nano-indentation measurements are shown in Fig.5 for 165 keV Ar ion and summarized in Table 2 for Cu and Au ions respectively.

Table 2: Comparison between the nano-hardness and Young's modulus values measured for unirradiated part and irradiated part for samples with 20 MeV Cu ion and, 3 MeV and 20 MeV Au ion.

Dose **Dpa**	Young's modulus GPA	Nano-hardness (GPA)	Micro-hardness (GPA)
Cu/20 MeV			
Unirradiated part	81.5± 0.9	1.58± 0.04	1.22±0.01
1dpa	81.5±1.4	1.62±0.04	1.29±0.02
Cu/0.7			
Unirradiated part	82.3±2.5	1.65±0.08	1.17±0.04
1.4 dpa	82.4±1.8	1.68±0.07	1.25±0.03
Au/3			
Unirradiated part	81.7 ±1.4	1.67±0.05	1.21±0.06
4.7 dpa	86.5±1.4	1.72±0.07	1.3±0.04
Au/20			
Unirradiated part	83.8 ±2.1	1.58±0.03	1.22±0.04
2.8 dpa	80±0.9	1.61 ±0.06	1.3±0.05

One can see that nano-hardness and Young's modulus increase a little bit in the case of 165 keV Ar and 3 MeV Au ions for which the probed length is similar to the ion path in Al6061. While both parameters remain unchanged in the case of the 20 MeV Cu ion and the 20 MeV Au ion as expected, since the probed length is limited to the shallow layer below 500 nm where the nuclear collision mechanism is negligible. As known, such mechanism is dominant at the end of the ion path. Table 2 report the comparison between the nano-hardness and Young's modulus values measured for unirradiated part and irradiated part with 20 MeV Cu ion and, 3 MeV and 20 MeV Au ion.

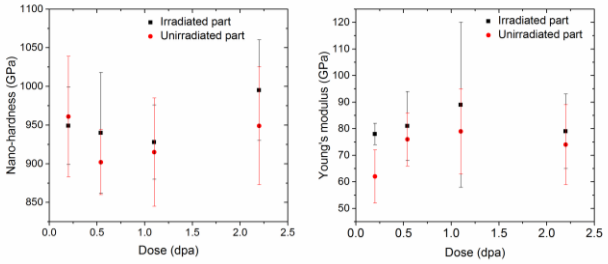

Fig. 5. Comparison between the nano-hardness and Young's modulus values measured for unirradiated part and irradiated part with 165 keV Ar ion.

4. Conclusion

Radiation damage induced in Al6061 by different ions species in the dose range up to 23 dpa was investigated using grazing X-ray diffraction, micro- and nano-indentation techniques. XRD data reveal the extinction of all diffraction line after irradiation at high dose except the peak (200) which persists even at high dose. According to

our data, this is due to the new phases and precipitates formation. Good correlation is found between the I(200)/I(111) peak ratio and nuclear stopping power indicating that nuclear collision mechanism is responsible of defect formation in metallic alloys. These damage, mainly vacancy and interstitial clusters, affect the grain size, micro-strain and peaks shift which increase/or decrease depending on the ion species and dose. It is found that the micro-hardness increases a little bit after irradiation indicating Al6061 hardening by ion beam irradiation. These results demonstrated that Al6061 structure and microstructure is considerably affected by swift heavy ion (equivalent fission fragments) irradiation which probably influences the mechanical properties. Therefore, taking into account the results of the present study, the lifetime of Al6061 under nuclear reactor operation conditions should be reviewed.

Acknowledgements

Authors are indebted to the NCP Accelerator staff for ion beam irradiations

Conflict of Interest

The authors declare that they have no conflict of interest

References

1. Kolobneva LI. Metallurgical Approach to Creation of Structural Aluminum Alloys for Nuclear Reactors*; Metal Science and Heat Treatment* .2004; 46: 474–478.
2. Farrell K. Performance of aluminum in research reactors. In: *Comprehensive Nuclear Materials* V5. Editor: Konings RJM, Elsevier; Oxford. 2012; 143–157.
3. Jin H J, Kim TK. Neutron irradiation performance of Zircaloy-4 under research reactor operating conditions. *Ann. Nucl. Energy*.2015; 75: 309–15
4. Farrell K, King R. Tensile Properties of Neutron-Irradiated 6061 Aluminum Alloy in Annealed and Precipitation-Hardened Conditions, ASTM, STP683-EB, *Effects of Radiation on Structural Materials*, Editor(s): J. A. Sprague, David Kramer, https://DOI:10.1520/STP38180S.
5. Flament C, Ribis J, Garnier J, Serruys Y, Leprêtre F, Gentils A, Baumier C, Descoins M, Mangelinck D, Lopez A, Colas K., Buchanan K, Donnadieu P. Alexis Deschamps, Stability of β'' nano-phases in Al-Mg-Si(-Cu) alloy under high dose ion irradiation, *Acta Materialia*, 2017, https://doi: 10.1016/j.actamat.2017.01.044
6. Ueyama D, Saitoh Y, Hori F, Kaneno Y, Nishida K, Dohi K, Soneda N, Semboshi S, Iwase A. Effects of energetic heavy ion irradiation on hardness of Al–Mg–Si alloys, *Nucl. Instr. and Meth. B.*2013; 314:107-111.
7. Ziegler JF, Ziegler MD, Biersack JP. SRIM - The Stopping and Range of Ions in Matter (2010). *Nucl. Instr. and Meth. B.* 2010; 268 (11–12): 1818–1823. https://doi.org/10.1016/j.nimb.2010.02.091.
8. Hengstler-Eger RM, Baldo P, Beck L, Dorner J, Ertl K, Hoffmann PB, Hugenschmidt C, Kirk M.A, Petry W, Pikart P, Rempel A. Heavy ion irradiation induced dislocation loops in AREVA's M5 alloy, *J. Nucl. Mater*. 2012; 423:170-182. doi:10.1016/j.jnucmat.2012.01.002.
9. Oliver W C, Pharr GM. An Improved Technique for Determining Hardness and Elastic Modulus Using Load and Displacement Sensing Indentation Experiments. *Journal of Materials Research*. 1992; 7(6): 1564–1583. https://doi.org/10.1557/JMR.1992.1564.
10. Belkacemi-Rebrab LT, Meslin E, Crocombette J-P, Radiguet B, Leprêtre F. Radiation-induced segregation/precipitation in Fe-Ni and Fe-Mn model alloys: Dose rate and solute effects. *J. Nucl. Mater*.2021; 548: 152807. https://DOI:10.1016/j.jnucmat.2021.152807.
11. San Chae, Yong-Soo Kim, Mohsin Rafique. Spectroscopic and microstructural characterization of 18 MeV He+ ions irradiated pure Al, *Optik*. 2016; 127: 9152–9160, https://doi.org/10.1016/j.ijleo.2016.06.130.

Recommended Citation

Izerrouken M, Sari A, Menchi O, Haid F, Ishaq A. Al 6061-T6 microstructure and mechanical properties modification under ion beam irradiation at room temperature: Application for Nuclear Research Reactor. *Alger. J. Eng. Technol. 2023*; 08(2):272-276. https:/dx.doi.org/10.57056/ajet.v8i2.133